The EMBO Journal (2004) 23, 3769–3779 | © 2004 European Molecular Biology Organization | All Rights Reserved 0261-4189/04
www.embojournal.org

THE EMBO JOURNAL

Protocadherin FAT1 binds Ena/VASP proteins and is necessary for actin dynamics and cell polarization

Marcus J Moeller[1,3], Abdulsalam Soofi[3], Gerald S Braun[1], Xiaodong Li[3], Carsten Watzl[2], Wilhelm Kriz[1] and Lawrence B Holzman[3,*]

[1]Institute for Anatomy and Cell Biology, University of Heidelberg, Heidelberg, Germany, [2]Institute for Immunology, University of Heidelberg, Heidelberg, Germany and [3]Department of Internal Medicine, University of Michigan Medical School, Ann Arbor, MI, USA

Cell migration requires integration of cellular processes resulting in cell polarization and actin dynamics. Previous work using tools of *Drosophila* genetics suggested that protocadherin fat serves in a pathway necessary for determining cell polarity in the plane of a tissue. Here we identify mammalian FAT1 as a proximal element of a signaling pathway that determines both cellular polarity in the plane of the monolayer and directed actin-dependent cell motility. FAT1 is localized to the leading edge of lamellipodia, filopodia, and microspike tips where FAT1 directly interacts with Ena/VASP proteins that regulate the actin polymerization complex. When targeted to mitochondrial outer leaflets, FAT1 cytoplasmic domain recruits components of the actin polymerization machinery sufficient to induce ectopic actin polymerization. In an epithelial cell wound model, FAT1 knockdown decreased recruitment of endogenous VASP to the leading edge and resulted in impairment of lamellipodial dynamics, failure of polarization, and an attenuation of cell migration. FAT1 may play an integrative role regulating cell migration by participating in Ena/VASP-dependent regulation of cytoskeletal dynamics at the leading edge and by transducing an Ena/VASP-independent polarity cue.

The EMBO Journal (2004) **23,** 3769–3779. doi:10.1038/sj.emboj.7600380; Published online 2 September 2004
Subject Categories: cell & tissue architecture; development
Keywords: actin dynamics; cellular migration; FAT1; planar cell polarity; VASP

Introduction

Mammalian FAT1 is a large transmembrane protein of the protocadherin superfamily first identified in *Drosophila melanogaster* (Mahoney *et al*, 1991; Wu and Maniatis, 2000). A number of studies in *Drosophila* implicated fat in the establishment of cell polarity in the plane of tissues ('planar cell polarity') (Rawls *et al*, 2002; Yang *et al*, 2002; Ma *et al*, 2003), a process that in part has been suggested to require directed actin polymerization (Kaltschmidt *et al*, 2002). While FAT1 is widely expressed in mammalian tissues, it is particularly enriched in kidney glomerular epithelial cells (Dunne *et al*, 1995; Ponassi *et al*, 1999; Cox *et al*, 2000; Inoue *et al*, 2001; Mitsui *et al*, 2002). Also termed 'podocytes', glomerular epithelial cells have a complex cyto-architecture that includes abundant filopodia-like, actin filament-rich processes that form interdigitations with neighboring cells. Significantly, genetic deletion of FAT1 from mice resulted in developmental defects including failure of normal development of these actin-rich podocyte processes (Ciani *et al*, 2003). Given that these observations suggested a role for FAT1 in regulating actin dynamics, an investigation of FAT1 cell biology was undertaken.

*Corresponding author. University of Michigan Medical School, 1560 MSRB II, Ann Arbor, MI 48109-0676, USA. Tel.: +1 734 764 3157; Fax: +1 734 763 0982; E-mail: lholzman@umich.edu

Received: 17 March 2004; accepted: 3 August 2004; published online: 2 September 2004

Results

Characterization of two polyclonal FAT1 antisera

Two polyclonal FAT1 antisera were raised in rabbits against recombinant GST-FAT1 cytoplasmic domain or against a 20-amino-acid (aa) peptide near the C-terminus of FAT1. Both antisera and a previously characterized anti-FAT1 antiserum (Inoue *et al*, 2001) specifically recognized a protein obtained from NRK-52E cell lysates with mobility on SDS–PAGE consistent with its predicted molecular mass of 500 kDa (Figure 1A). The specificity of these antisera was confirmed in cells depleted of endogenous FAT1. NRK-52E cells were transiently cotransfected with plasmids encoding a rat FAT1-specific small hairpin RNA (shRNA) template and eGFP as a transfection marker. Specific reactivity of anti-FAT1 antisera was markedly reduced only in transfected NRK-52E cells (Figure 1B and B′).

FAT1 localizes at the plasma membrane at sites of actin polymerization

The subcellular localization of FAT1 was examined in epithelial NRK-52E and in neuronal HN33 cells by immunofluorescence (IF) and by immunoblotting cell lysates. In both cell lines, FAT1 localized to actin-based structures at the plasma membrane, including the leading edge of lamellipodia, filopodial protrusions, and the mature intercellular junction (Figure 2). In NRK-52E cells, FAT1 staining was mostly continuous along the entire lamellipodial leading edge (Figures 2A and 4C). In differentiated neuronal HN33 cells, FAT1 was enriched on microspike tips of lamellipodial protrusions (Figure 2C and D). FAT1 was also present along the tips and shaft of filopodial protrusions in a punctate pattern. Punctate staining was particularly obvious at the tips of short freshly emerging filopodial protrusions (Figure 2B–D) identified by phosphotyrosine labeling and by videomicroscopy prior to staining. FAT1 staining was also observed along the shaft of retraction fibers. FAT1 staining was present at mature

intercellular junctions but its distribution at these junctions was clearly distinct from that of classical cadherins (e.g. E-cadherin; Figure 2E–E″) or ZO-1 (not shown). Taken together, these observations suggested that FAT1 localized to sites of directed actin polymerization associated with the plasma membrane and was also found along shafts of filopodia and in retraction fibers.

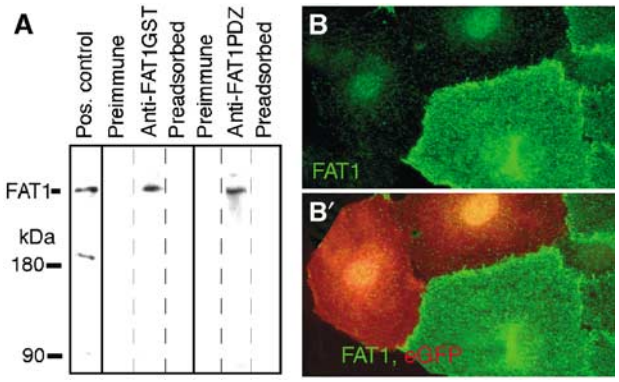

Figure 1 Characterization of FAT1 antisera. (**A**) NRK-52E cell lysates were separated by SDS–PAGE and immunoblotted with an affinity-purified antiserum raised against the FAT1 cytoplasmic domain (lanes 2–4) or a peptide from the COOH-terminus of FAT1 (lanes 5–7). A band of approximately 500 kDa was detected by both antisera and a previously characterized anti-FAT1 antibody (lane 1). (**B**) To demonstrate the specificity of the FAT1GST antiserum by indirect IF microscopy, endogenous FAT1 was knocked down with a FAT1-specific shRNA template in NRK-52E cells (FAT1, green) marked with cotransfected eGFP (merge, red).

FAT1 directly interacts with and colocalizes with VASP and Mena in cells

The FAT1 cytoplasmic domain contains a potential EVH1-binding motif ($_{4433}$DFPPPPEE) that is conserved among rodents and humans. EVH1-binding motifs are predicted to interact with EVH1 domain-containing proteins of the Ena/VASP protein family including Mena and VASP that function in the actin polymerization complex (Niebuhr *et al*, 1997; Bear *et al*, 2002). Indeed, in pulldown experiments, the VASP EVH1 domain interacted with the FAT1 cytoplasmic domain (Figure 3A).

To confirm this, we assessed the ability of the FAT1 cytoplasmic domain to recruit endogenous Ena/VASP proteins in cells. FLAG-tagged FAT1 cytoplasmic domain (FAT1mito) was targeted to the outer leaflet of mitochondria in transiently transfected cells using a C-terminal signal peptide from the *Listeria* protein ActA (Pistor *et al*, 1994; Fradelizi *et al*, 2001) (Figure 3B and B′). Recruitment of endogenous VASP by FAT1mito to mitochondria was assessed in these cells. Overexpression of FAT1mito invariably caused strong recruitment of endogenous VASP to the mitochondrial outer leaflet and depletion of endogenous VASP from the leading edge and focal contacts (Figure 3C and D). Mena recruitment occurred in a similar fashion (not shown). In untransfected COS-7 cells, mitochondria labeled with a vital dye were located in a loose perinuclear cluster. Unexpectedly, mitochondria in transfected cells were condensed into aggregates and were displaced away from the cell nucleus into the periphery of the cells (see below). In COS-7 cells, FAT1mito-decorated mitochondria were often detected at the tip of cellular processes (Figure 3B–D).

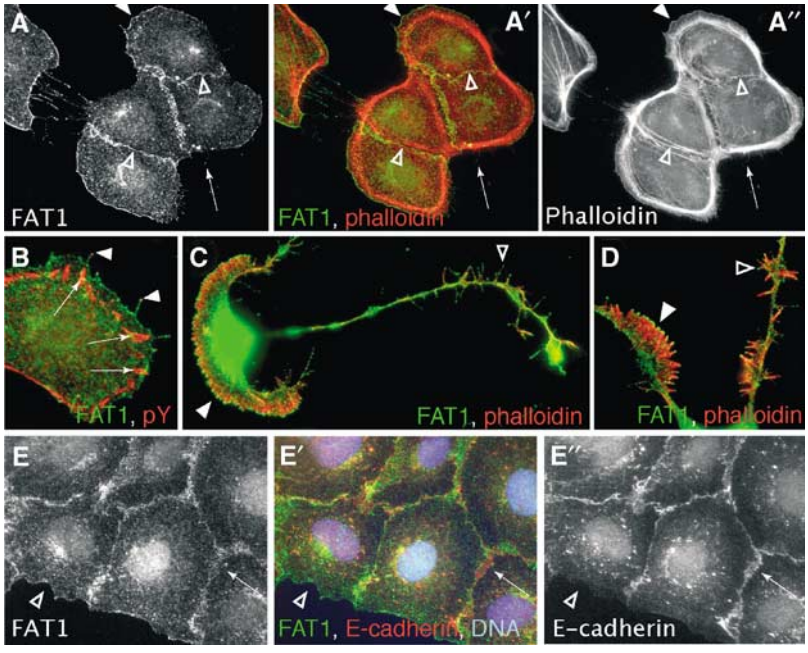

Figure 2 Cellular localization of endogenous FAT1. (**A, A′, A″**) FAT1 was enriched in NRK-52E cells at the leading edge of lamellipodial protrusions (solid arrowhead), at intercellular junctions (arrowheads), and along actin-based filopodial protrusions in a punctate pattern (arrow). (**B**) FAT1 was present along the shaft and the tips of filopodial protrusions marked by phosphotyrosine (pY) (arrowheads) but not in focal adhesions (arrows). (**C**) FAT1 at the tips of microspikes along lamellipodial protrusions (full arrowhead) and the tips of filopodial protrusions (empty arrowhead) in differentiated neuronal HN33 cells. (**D**) Higher magnification of a differentiated HN33 cell demonstrating FAT1 localization at the tips of actin-based microspikes and filopodial protrusions. (**E–E′**) FAT1 did not entirely colocalize with classical cadherins (E-cadherin) along the intercellular junction in NRK-52E cells (arrow). No classical cadherins were observed along the free edge of cells (arrowhead).

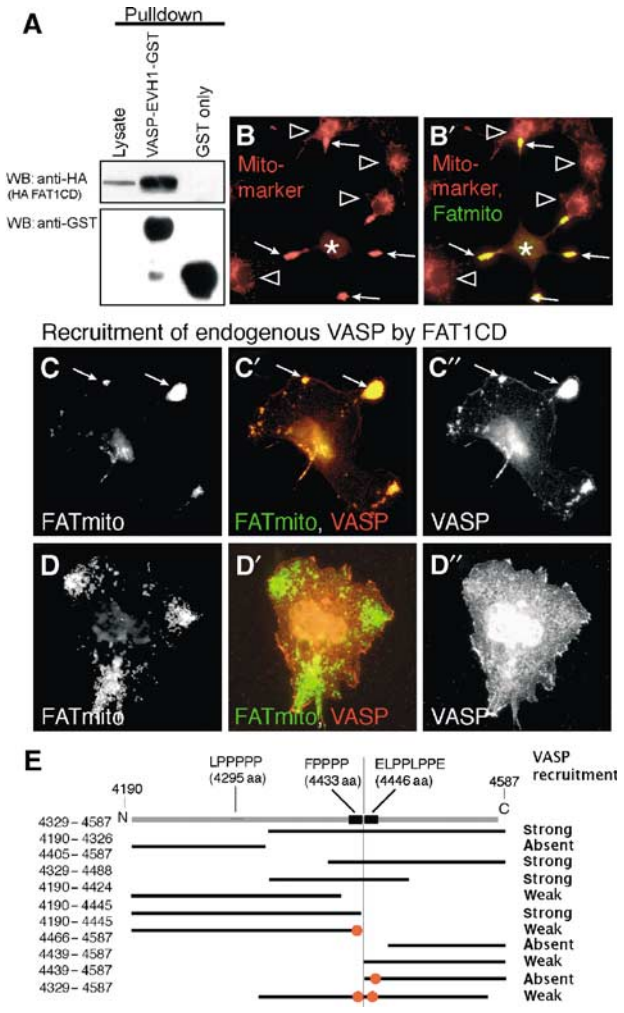

Figure 3 FAT1 binds to and recruits Ena/VASP proteins. (**A**) HA-tagged FAT1 cytoplasmic domain expressed in COS 7 cells was pulled down using bacterially expressed recombinant GST-VASP-EVH1 domain (anti-HA immunoblot). Lysate for each pulldown was loaded in lane 1 to show input. The quantity of GST fusion protein was visualized (anti-GST immunoblot). (**B, B′**) FLAG-tagged cytoplasmic domain of FAT1 coupled to a mitochondrial targeting signal peptide (FAT1mito) was targeted to the outer leaflet of mitochondria in COS-7 cells (*) (mitochondria labeled with MITO-MARKER red®). Expression of FAT1mito invariably caused mitochondrial displacement into cellular processes (arrows) not seen in untransfected COS-7 cells (empty arrowheads). (**C, D**) Representative experiments in which COS-7 cells were transfected with FAT1mito and in which endogenous VASP recruitment to mitochondria was evaluated (red, endogenous VASP; green, FAT1mito and its deletion mutants identified with anti-FLAG antibody, arrows). (C) Wild-type full-length FAT1 cytoplasmic domain (FAT1mito). (D) FAT1mito(4190–4326). (**E**) Schematic of FAT1 cytoplasmic domain deletions/point mutants used to map functionally relevant VASP-binding sites. Indicated mutants were targeted to the outer leaflet of mitochondria in COS-7 cells. IF microscopy was used to evaluate the capacity of FAT1mito mutants to recruit endogenous VASP to mitochondria and to deplete endogenous VASP from its typical distribution within cells. As indicated in the schematic, ability of mutants to affect VASP cellular distribution was described as strong, weak, or absent according to a scoring system in Materials and methods.

A series of deletion mutants fused to the mitochondrial targeting motif were created and were used to map regions within the FAT1CD capable of recruiting endogenous VASP (summarized in Figure 3E). FAT1 deletion mutant 4329–4488 aa was sufficient to mediate strong recruitment of endogenous VASP to mitochondria. Within this region, two proline-rich motifs were identified. One of these sites, $_{4433}$DFPPPPEE, matched the previously identified conserved EVH1-binding domain motif (Niebuhr *et al*, 1997). A second motif ($_{4446}$ELPPLPPE) had not been previously described. The former domain recruited endogenous VASP and Mena with higher affinity than the latter. Of note, while these domains are highly conserved among higher vertebrates, they are not conserved in *D. melanogaster*. A third domain located between residue 4329 and 4405 appeared to be sufficient for weak recruitment of endogenous VASP.

Pulldown experiments and Farwestern overlay experiments were used to confirm that the FAT1CD proline-rich motifs identified in the previous recruitment experiments mediated an interaction with VASP and Mena. FAT1 cytoplasmic domain pulled down VASP and Mena obtained from NRK-52E cell lysates (Figure 4A). This interaction was attenuated by introducing point mutations in either of the two proline-rich regions of the predicted EVH1-binding motifs; simultaneous point mutations in both proline-rich motifs were required to entirely extinguish these interactions. Farwestern analysis confirmed that recombinant GST-VASP-EVH1 domain bound directly to wild-type FAT1 cytoplasmic domain (Figure 4B). In agreement with the results described above, the interaction detected by Farwestern blotting was attenuated by point mutations in either proline-rich domain or was abolished by mutations in both proline-rich domains.

In additional studies, FAT1 colocalized with Mena and VASP in actin-based structures at the plasma membrane in the cell lines studied (Figure 4C). Because VASP fused to eGFP (VASP-GFP) was previously described to localize in cells in a fashion similar to endogenous VASP (Vasioukhin *et al*, 2000), NRK-52E cells were transiently transfected with VASP-GFP. Here, VASP-GFP colocalized with endogenous FAT1 at the leading edge of lamellipodial protrusions and at mature intercellular junctions. No colocalization of VASP-GFP and FAT1 was seen at focal contacts, where endogenous FAT1 was absent. Colocalization of endogenous FAT1 and Mena was also observed at the tips of microspikes of differentiated neuronal HN33 cells (not shown).

Ectopic actin polymerization on FAT1mito-decorated mitochondria

Since VASP and Mena participate in the actin polymerization complex, we examined whether expression of FAT1mito resulted in ectopic actin polymerization. Importantly, phalloidin staining suggested the presence of filamentous actin around mitochondria of FAT1mito-transfected COS-7 cells (Figure 5A–A″). As described previously by Fradelizi *et al* (2001), expression of zyxin-NT targeted to the outer leaflet of mitochondria in transiently transfected cells served as positive control and demonstrated robust phalloidin staining at this site (Figure 5B–B″). Of note, mitochondrial phalloidin staining induced by expression of FAT1mito was significantly weaker in comparison to that induced by zyxin-NT and was observed only in cells with abundant expression of FAT1mito. These observations suggested that the ectopic expression of FAT1 cytoplasmic domain recruited a complex of proteins sufficient to induce actin polymerization. In fact, endogenous Arp3 (not shown) or cotransfected Arp3-GFP was recruited to

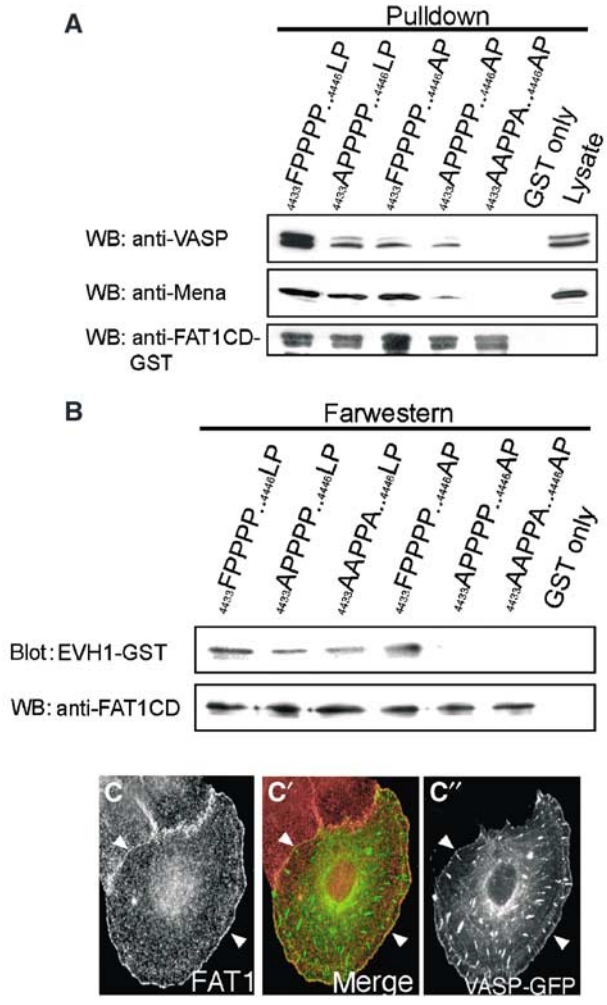

Figure 4 FAT1 binds to and colocalizes with VASP and Mena via two EVH1-binding domains. (**A**) Endogenous VASP and Mena were pulled down from NRK-52E cell lysates using indicated recombinant mutants of the GST-FAT1 cytoplasmic domain. Point mutations were introduced at the identified EVH1-binding regions (FPPPP at position 4433 aa and ELPP at 4446 aa). Lane 7 was loaded with input cell lysate. Equal loading was verified by stripping membranes and reimmunoblotting for FAT1. (**B**) Farwestern assay demonstrated that the EVH1 domain of VASP binds directly to two EVH1-binding sites identified. FAT1-GST cytoplasmic domain mutants were separated by SDS–PAGE, transferred to a nitrocellulose membrane, and probed with radiolabeled GST-VASP-EVH1 domain. (**C, C′, C″**) NRK-52E cell transiently transfected with VASP-GFP. Colocalization of endogenous FAT1 and VASP-GFP was seen at the leading edge and intercellular junction (solid arrowheads). Unlike VASP-GFP, FAT1 was not present at focal contacts. WB, immunoblot; blot, Farwestern overlay.

mitochondria by FAT1mito expression (Figure 5C–C″). Actin-associated proteins including endogenous cortactin, N-WASP, and alpha-actinin were also recruited by FAT1mito. No significant mitochondrial recruitment of endogenous vinculin or ZO-1 was observed (not shown). Because published work on the *Listeria* protein ActA showed that recruitment of the Arp2/3 complex occurs independently of VASP, we investigated whether Arp3 recruitment to FAT1 occurs independently of the FAT1 EVH1-binding domain. Indeed, when expressed in COS7 cells, a FAT1 mutant deleted of its EVH1 interaction domain continued to recruit Arp3-GFP (Figure 5D–D″).

Impaired wound closure in FAT1-deficient NRK-52E monolayers

That FAT1 is a transmembrane protein associated with VASP and/or Mena at sites of actin polymerization suggested the hypothesis that FAT1 is necessary for regulation of cell motility. To investigate this hypothesis, an *in vitro* wound model was employed in which scrape wounds were made across a confluent monolayer of NRK-52E cells. In this model, cells at wound edges become polarized and form lamellipodia at the cellular leading edge that extend into the denuded space. Subsequently, the entire monolayer moves forward in a coordinated fashion perpendicular to the direction of the open wound (Nobes and Hall, 1999). To investigate if FAT1 is necessary for normal cell migration in this system, FAT1 expression was attenuated using RNA interference (RNAi). Monolayers were transduced either with control lentivirus or lentivirus expressing a FAT1-specific shRNA template (FAT1KD) in paired experiments (Figure 6A and B). Viral supernatants of FAT1KD were titered to achieve attenuation of endogenous FAT1 expression in about 90% of cells. Attenuation of FAT1 expression by RNAi in monolayers was confirmed by immunoblotting (Figure 6C). Within the pool of FAT1KD-transduced cells, FAT1 expression was variably attenuated; as discussed below, this heterogeneity proved experimentally useful. Standard wounds—made with either a 200 μl pipette tip or a 1 ml pipette tip—reproducibly measured 390 μm across (s.d. $\pm$44 μm; based on 10 measurements made every 340 μm along a wound in four independent experiments) or 590$\pm$52 μm, respectively. Time to wound closure was measured until 50% of the entire length of the wound first attained closure. Control lentivirus expressing eGFP without a FAT1 shRNA did not affect the rate of wound closure. Compared to vector control, the rate of wound closure was dramatically impaired in NRK-52E monolayers transduced with FAT1KD virus in nine paired experiments (Figure 6D).

Observation by videomicroscopy of wounds made in NRK-52E monolayers transduced with FAT1KD suggested that coordinated migration of the monolayer into denuded wounds occurred at infrequent sites led by polarized cells (Figure 6B and E). These 'leader cells' were defined experimentally as localized protrusions into the denuded area of more than two cell diameters. Interestingly, a mean of 88$\pm$5% of leader cells located at the tip of these cellular protrusions expressed endogenous FAT1. Cells trailing FAT1-positive leader cells followed leader cells forward in a coordinated fashion even when these trailing cells lacked FAT1 (Figure 6E and E′). In contrast, FAT1-deficient cells at the wound edge typically appeared nonpolarized even when these FAT1-deficient cells were adjacent to FAT1-expressing leader cells (data not shown). Transduction with control virus did not affect the ability of cells to become leader cells (not shown). These results show that FAT1 is necessary for normal cell migration in an *in vitro* wound model.

FAT1-negative cells at the leading edge have impaired lamellipodial dynamics

Impaired cellular motility and the delay in wound closure in FAT1-deficient NRK-52E cell monolayers could be a consequence of impaired actin dynamics at the leading edge or a polarity defect or both. To test the first hypothesis, lamellipodial dynamics were evaluated by IF and phase-contrast videomicroscopy in cells along the wound edge of control or

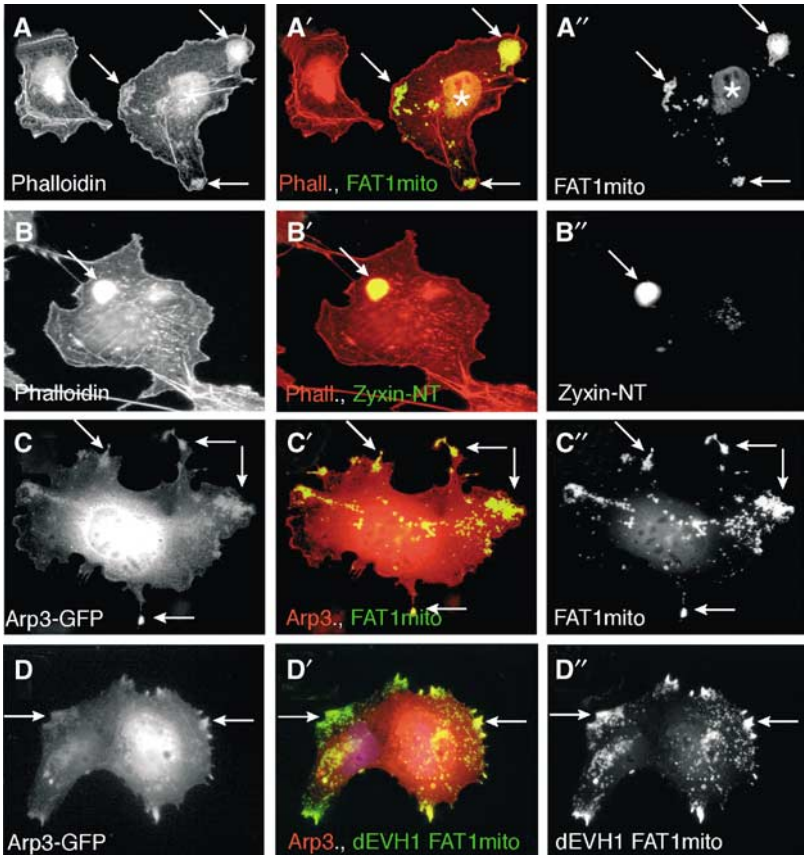

Figure 5 FAT1mito expression is sufficient to recruit components of the actin polymerization complex and to induce ectopic actin polymerization. (**A, A′, A″**) Overexpression of the FAT1 cytoplasmic domain (FAT1mito) on the outer leaflet of mitochondria in a transiently transfected COS-7 cell (*) was sufficient to induce ectopic actin polymerization (arrows). (**B, B′, B″**) Expression of the N-terminal portion of zyxin (zyxin-NT) on mitochondria of COS-7 cells nucleated ectopic actin polymerization. (**C, C′, C″**) Mitochondrial recruitment (arrows) of Arp3-GFP was detected in COS-7 cells also expressing FAT1mito. (**D, D′, D″**) Similarly, weak Arp3-GFP recruitment is shown in two transiently transfected cells expressing FAT1mito lacking EVH1-binding domains (dEVH1 FAT1mito).

FAT1KD-transduced NRK-52E monolayers at 5 and 16 h after wounding (Figure 7). In general, cells with attenuated expression of FAT1 had absent or abnormal appearing lamellipodia with decreased lamellar size and abnormal structure. Subjectively, there appeared to be a relationship between the degree of attenuation of FAT1 expression and the degree to which lamellipodia formation was impaired (Figure 7A and A′). Quantitatively, lamellipodia formation (defined as present if more than 50% of the wound edge of the cell was occupied by a lamellipodial protrusion *irrespective* of lamellipodial morphology) was compared in FAT1-positive and FAT1-deficient cells (Figure 7B). In cells transduced with control virus, about 55% of wound edge cells had formed lamellipodia at 5 h after wounding; by 16 h, 90% of wound edge cells were lamellipodia positive. In contrast, in monolayers transduced with FAT1KD, less than 40% of FAT1-deficient cells formed lamellipodia 5 h after wounding. This defect in lamellipodia formation became more apparent 16 h after wounding since only about 50% of FAT1-deficient cells formed lamellipodial protrusions by this time point. Strikingly, the subpopulation of cells in FAT1KD-transduced monolayers with preserved FAT1 expression formed normal appearing lamellipodia with a frequency similar to cells transduced with control virus.

The abnormal appearance of lamellipodia noted above in NRK-52E monolayers transduced with FAT1KD was further evaluated. Using time-lapse videomicroscopy and kymography (Hinz *et al*, 1999), lamellipodial kinetics were impaired in leading edge cells of FAT1KD-transduced monolayers (Figure 7C–G). Most strikingly, these cells formed dramatically more ruffles at their leading edges observed per unit time and per protrusion. It was concluded that FAT1 is necessary for normal lamellipodial dynamics and that—at least in part—disruption of normal lamellipodial dynamics by FAT1 knockdown provides an explanation for attenuated cell migration in FAT1-deficient cells.

Because FAT1 recruited endogenous Ena/VASP proteins when ectopically targeted within cells and because recruitment of Ena/VASP to the leading edge has been implicated as regulating actin dynamics (Bear *et al*, 2002; Samarin *et al*, 2003), we tested whether endogenous FAT1 is necessary for the recruitment of endogenous Ena/VASP proteins to the leading edge. Line intensity scans were used to quantify the abundance of endogenous VASP at the leading edge in wild-type cells and in those in which FAT1 expression is attenuated by RNAi. Rottner *et al* (1999) showed that VASP was present at the leading edge only in protruding lamellipodia and not in those that were retracting. Moreover, it was noted that the abundance of VASP at the membrane was linearly proportional to the velocity of lamellipodial protrusion. Because of the heterogeneous nature of knockdown efficiency in the *in vitro* wound model employed here, we chose to quantify

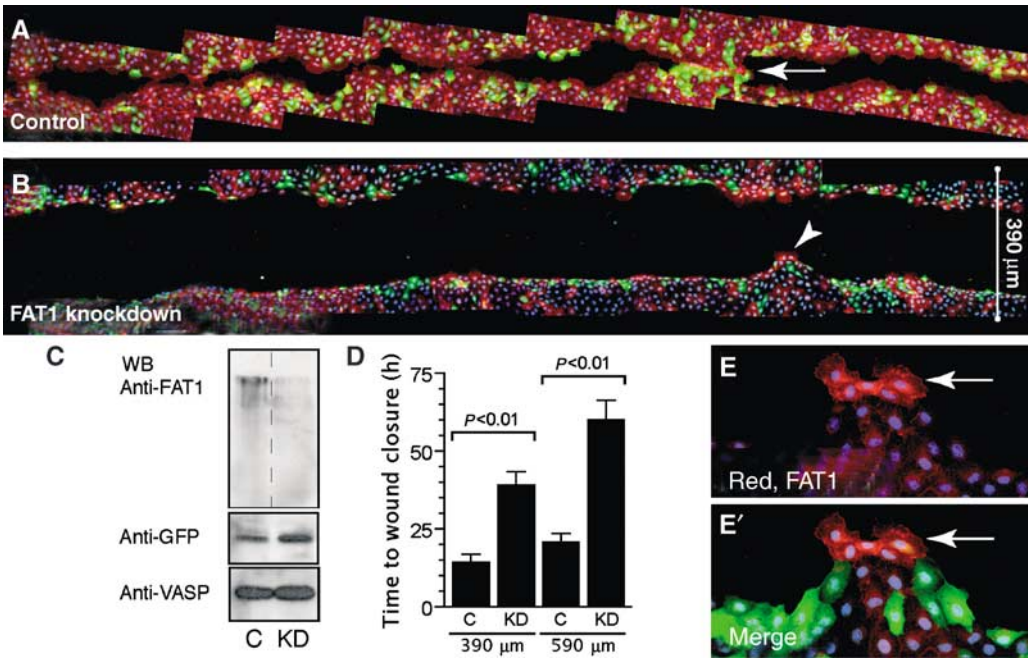

Figure 6 Delayed wound closure in FAT1-deficient NRK-52E cell monolayers. Confluent NRK-52E cells were transduced with control virus lentilox 3.7 (**A**) or with virus containing an shRNA template specific for FAT1 (FAT1KD) (**B**) 60 h prior to application of scratch wounds. After 16 h, cells were fixed and FAT1 (red), GFP (green), and nuclei (blue) were visualized by IF. Despite variable expression of eGFP, lentivirus transduction efficiency was between 80 and 90% in these experiments. Wound width at time = 0 is indicated as a white line on the right. Occasional cellular protrusions were led by FAT1-positive cells ('leader cells', arrowhead and at other sites in these photomicrographs). (**C**) Lysates of NRK-52E cells transduced with FAT1KD (KD) or control lentivirus bearing the GFP reporter only (C) were immunoblotted for endogenous FAT1 expression 60 h after transduction. Similar expression of the GFP reporter demonstrates comparable viral transduction. Immunoblotting for endogenous VASP demonstrated equal loading. (**D**) Representation shows delayed wound closure of NRK-52E monolayers transduced with control (C) versus FAT1KD (KD) virus. Values represent mean time to wound closure ± s.d. of nine independent paired experiments. *P*-value, paired Student's *t*-test. (**E, E′**) In NRK-52E cells transduced with FAT1KD heterogeneously expressing FAT1, wound closure was predominantly led by polarized cells with preserved FAT1 expression located at the tip of cone-shaped cellular protrusions (arrowhead; red, FAT1; green, GFP; blue, dsDNA). FAT1-deficient cells trailed immediately behind these 'leader cells' at a rate significantly faster than adjacent FAT1-negative cells.

the relative mean abundance of VASP at the leading edge. It was reasoned that this mean value would also account for average protrusion velocity and protrusion/retraction frequency. Three random areas on each cellular leading edge in multiple randomly selected cells along the wound edge were analyzed and a mean VASP IF intensity was obtained for each condition (Figure 7H). In cells at the leading edge transduced with the FAT1 shRNA encoding virus, we found that VASP abundance at the leading edge was reduced on average by approximately two-fold. However, FAT1 depletion did not result in complete failure of VASP recruitment to the leading edge. Therefore, FAT1 is not independently sufficient for recruitment of VASP to the leading edge; however, FAT1 is necessary in part to achieve *normal* targeting of VASP to this site.

FAT1 is necessary for the establishment of cellular polarity in the wound model

Polarization of cells directed toward the denuded space in the plane of the monolayer is an early event following denudation in the wound model; here polarization and cell migration are inter-related (Nobes and Hall, 1999). Because FAT1 was found to be required for normal cell motility in the previous experiments, the necessity of FAT1 for polarization of leading edge cells was investigated. The polarization of migrating cells in the wound model requires the reorganization of the microtubular network and is associated with the alignment of the microtubule organizing center (MTOC) in the direction of movement (Bershadsky and Futerman, 1994). In a confluent stationary monolayer, MTOCs are typically observed in close association with the Golgi apparati in a random orientation relative to the nucleus. In a wound assay, both structures become oriented toward the forward facing aspect of polarized leading edge cells (Nobes and Hall, 1999). Similarly in our hands, Golgi apparati (approximately 75% at 16 h postinjury) and MTOCs (approximately 60% at 6 h postinjury) became oriented within the forward facing sector of control NRK-52E leading edge cells after wounding the monolayer (Figure 8). In contrast, Golgi apparati and MTOCs of FAT1-deficient cells were found in a random distribution relative to the nucleus, suggesting that FAT1 is necessary for the establishment of cell polarity in the plane of the monolayer in this model.

FAT1mito-decorated mitochondria are dislocated in a polarized fashion independently of functional FAT1 EVH1-binding domain

FAT1mito was targeted to the mitochondrial outer leaflet in confluent NRK-52E monolayers using a lentiviral expression plasmid (wtFAT1mito). At 48 h post-transduction, the monolayer was wounded and analyzed (Figure 9). Interestingly, FAT1mito-decorated mitochondria in transduced cells at the

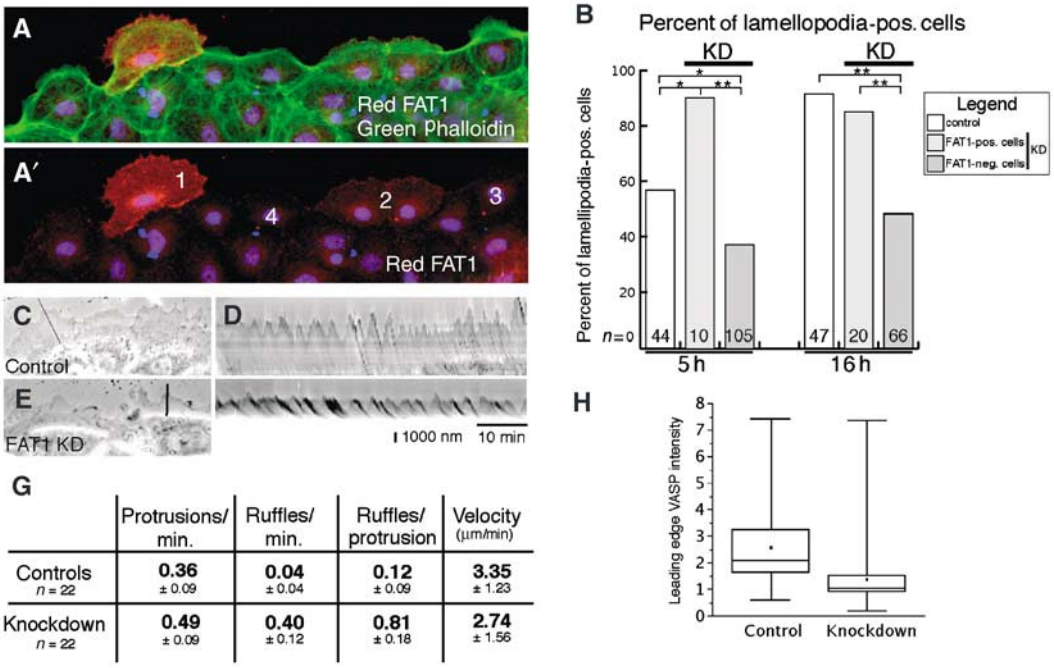

G

	Protrusions/ min.	Ruffles/ min.	Ruffles/ protrusion	Velocity (μm/min)
Controls $n = 22$	**0.36** ± 0.09	**0.04** ± 0.04	**0.12** ± 0.09	**3.35** ± 1.23
Knockdown $n = 22$	**0.49** ± 0.09	**0.40** ± 0.12	**0.81** ± 0.18	**2.74** ± 1.56

Figure 7 FAT1-deficient cells exhibit abnormal lamellipodial dynamics. (**A, A′**) FAT1KD-transduced cells along a wound edge 5 h after wounding exhibiting different degrees of FAT1 attenuation (cell 1, no attenuation; cell 2, intermediate attenuation; cells 3 and 4, nearly complete attenuation of FAT1; red, FAT1; green, f-actin; blue, dsDNA). (**B**) Comparison of prevalence of lamellipodia formation in leading edge cells expressing FAT1 and in those with attenuated FAT1 expression. Lamellipodia formation along the wound edge was evaluated in cells transduced with control and FAT1KD virus (KD) 5 and 16 h after wounding in three independent experiments. Lamellipodial protrusions were identified by phalloidin staining. Cells were counted as lamellipodia positive if more than 50% of their free aspect was occupied by a lamellipodial protrusion irrespective of lamellipodial morphology (e.g. cells 1, 2, and 3 in panels A and A′). *n*, total number of evaluated cells; ANOVA $P<0.05$. Nonoverlapping 95% confidence intervals are indicated by asterisks; nonoverlapping 99% confidence intervals are indicated by double asterisks. (**C–G**) Individual frames (C, E) and associated composite kymographs (D, F) from time-lapse movies of control-transduced (C, D) or FAT1KD-transduced (E, F) NRK-52E cells. Kymographs evaluate lamellipodial dynamics along the lines drawn on associated phase-contrast images. Ascending and descending contours of the edge indicate protrusion and withdrawal events, respectively. Dark shades observed during withdrawal events correspond to ruffles. (G) Individual protrusion and ruffling events per minute were counted in 22 cells (9–30 protrusion events each) in 11 time-lapse movie experiments.. Ruffling occurred significantly more often during withdrawal of lamellipodial protrusions in FAT1-deficient cells (ANOVA $P<0.01$). (**H**) Whisker plots describing leading edge VASP intensity. Leading edge VASP intensity was obtained at three sites in 30 cells from both knockdown and control leading edges. Dot represents mean, middle line of box indicates median, top of box indicates 75th quartile, bottom of box indicates 25th quartile, and whiskers indicate the extent of 10th and 90th percentiles, respectively. Unpaired, two-tailed *t*-test, $P<0.01$.

wound border were displaced in a highly polarized fashion toward the leading edge. Polarization of FAT1mito-decorated mitochondria occurred independently of Ena/VASP–FAT1 interaction since mitochondria in cells expressing FAT1mito deleted of the FAT1 EVH1-binding domain (dEVH1FAT1mito) no longer recruited endogenous VASP while they continued to translocate to the leading edge (Figure 9D–D″). Conversely, mitochondria in cells transduced with a mutant of FAT1mito lacking the N-terminal portion of FAT1 cytoplasmic domain proximal to the EVH1-binding domain (C-termFAT1mito) strongly recruited VASP but were not displaced (Figure 9E–E″). These experiments suggested that the FAT1 cytoplasmic domain interacts via a motif present in its N-terminus—and independently of an interaction with Ena/VASP—with a complex of proteins that respond to a polarity cue in the plane of the monolayer.

Discussion

The results presented suggest that FAT1 serves as a proximal element of signaling pathways necessary for cell migration that determine *both* cell polarity in the plane of the monolayer and directed actin-dependent cell motility. Unlike classical cadherins, FAT1 is located within cells at sites of high actin turnover including the leading edge of lamellipodia and filopodial protrusions. FAT1 colocalizes and directly interacts with VASP and Mena at these sites. Members of the Ena/VASP protein family regulate actin dynamics and influence actin-based cellular processes including axon guidance, lamellipodial dynamics, and cell motility (Rottner *et al*, 1999; Bear *et al*, 2002; Samarin *et al*, 2003). The conclusion that FAT1 participates in regulating actin dynamics is strengthened by the observations that artificially targeted FAT1 cytoplasmic domain recruited a protein complex sufficient to induce ectopic actin polymerization, that FAT1 is necessary for normal recruitment of VASP to the leading edge, and that attenuating FAT1 expression impaired cellular processes dependent on normal actin dynamics.

The mechanism by which FAT1 affects actin dynamics remains to be fully elucidated. FAT1 may serve both as a scaffold that binds Ena/VASP proteins at the leading edge and as a receptor that transduces extracellular cues to regulate the Ena/VASP-containing complex. FAT1 may also provide a scaffold for the recruitment of additional proteins necessary for actin polymerization including the Arp2/3 complex. Independently, FAT1 is not sufficient for recruitment of

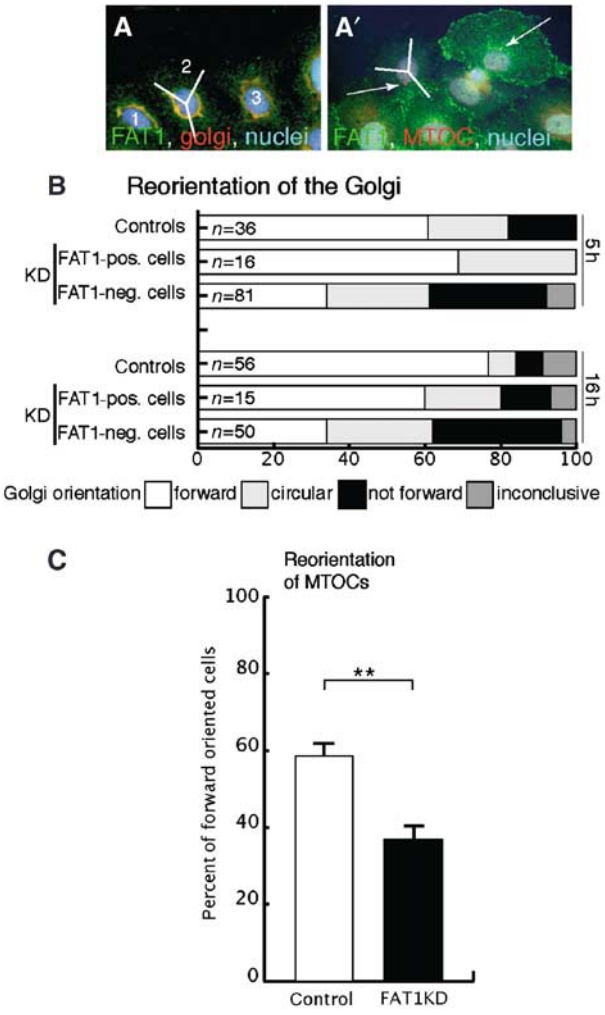

Figure 8 FAT1 is necessary to establish planar polarity in the wound model. (**A**) Leading edge planar polarity was evaluated in FAT1KD- and control virus-transduced wounded monolayers by evaluating the polarity of Golgi apparati (A) and microtubule organizing centers (MTOC's, A′) in these cells. Immunostained cells were divided into three 120° sectors as shown and the polarity of Golgi apparati or MTOCs relative to the wound edge were quantified (green, Golgi apparatus or MTOC; red, FAT1). In the examples shown in panel A, the Golgi in cell marked 1 is located in the forward facing sector, while the Golgi in cells marked 2 is not in the forward sector; cells—like that marked 3—with no apparent polarization of the Golgi apparatus were classified as 'circular'. (**A′**) Similarly, MTOC (arrows) is not polarized toward the leading edge in FAT1-deficient cells and is appropriately polarized in FAT1-positive cells. (**B**) The distribution of Golgi relative to the wound edge was tabulated 5 and 16 h after wounding. (**C**) The orientation of MTOCs relative to the leading edge was quantified in FAT1-deficient cells (FAT1KD) 5 h after wounding (**; $P<0.01$ χ^2 test, $n=600$). A nonpolarized cell population would be expected to exhibit a random distribution of the Golgi apparatus or MTOC relative to the wound edge in which 33% of Golgi/MTOCs were present in the forward sector.

endogenous VASP to the leading edge; however, FAT1 is required to obtain normal VASP abundance at this site. This conclusion is consistent with the conclusion of Bear *et al* (2002), who noted that VASP recruitment to the leading edge is mediated by a combination of interactions involving both the EVH1 and EVH2 domains of Ena/VASP proteins. When expressed independently of the EVH1 domain, the barbed end binding EVH2 domain was localized to the actin network within lamellipodia but was not detected at the leading edge. In contrast, the Ena/VASP EVH1 domain alone was weakly targeted to the leading edge. The observations herein suggest that FAT1 represents a previously unidentified EVH1-binding domain-containing transmembrane protein that binds the EVH1 domain of Ena/VASP proteins and contributes with other interactions to determine appropriate Ena/VASP targeting.

The observation that FAT1 is also necessary for the establishment of polarity in the plane of the monolayer of leading edge cells is consistent with a role established for *Drosophila* fat. This work identified *Drosophila* fat as a necessary component of a signaling mechanism that establishes planar cell polarity in polarized tissues including the compound eye and wing (Yang *et al*, 2002; Ma *et al*, 2003). Genetic analysis suggested that fat interacts with protocadherin dachsous via an intercellular heterotypic interaction that transmits positional cues to frizzled (Ma *et al*, 2003). Details of the molecular mechanisms by which planar cell polarity cues are transduced to the cell remain incompletely understood. The results reported here identify mammalian FAT1 as a necessary element of a pathway that determines polarity in the plane of the monolayer. The results of the FAT1mito mitochondrial targeting assay in the context of the wound model are consistent with our findings obtained by RNAi and suggest the hypothesis that the FAT1 cytoplasmic domain interacts with a yet to be identified complex of proteins involved in cellular polarity. Importantly, the interaction between FAT1 and Ena/VASP proteins was not necessary to affect the polarized distribution of FAT1mito-decorated mitochondria in these experiments.

During the revision of this manuscript, Tanoue and Takeichi (2004) published observations that are generally confirmatory of, or complementary to, the results reported herein. These investigators reached similar conclusions that FAT1 binds Ena/VASP proteins and is necessary for normal actin dynamics and cell polarization. Most importantly, the observations made herein emphasize that FAT1 appears to play an integrative role in regulating cell migration by participating in the regulation of actin dynamics at the leading edge, by recruiting additional proteins involved in actin polymerization independent of Ena/VASP, and by transducing an Ena/VASP-independent polarity cue.

Materials and methods

Plasmid constructs

Plasmid constructs were prepared by standard PCR cloning techniques and were subsequently DNA sequenced (Moeller *et al*, 2002). The full-length cytoplasmic domain of murine FAT1 was isolated from cDNA clones (gift of Dr T Magee; Cox *et al*, 2000) and IMAGE clone #4486159 (GenBank Acc#: BG243636). FAT1mito or its truncation mutants were constructed by cloning the mitochondrial targeting sequence of ActA obtained from the 3′ 78 bp of the zyxin-NT coding region (gift of Dr RM Golsteyn; Fradelizi *et al*, 2001) into the *Xba*I/*Bam*HI sites of p3xflag-CMV-10 (#E-4401, Sigma). Subsequently, the full-length FAT1 cytoplasmic domain (aa 4190–4587, all amino-acid positions are referenced to GenBank Acc#: AJ250768) or its truncation mutants were inserted into the *Hin*dIII/*Xba*I sites in the same vector. 3xflag-tagged FAT1 cytoplasmic domain and its mutants were shuffled into pLenti6/V5-D-TOPO (Invitrogen) using the following primers: forward 5′CAC CAT GGA CTA CAA AGA C3′ and reverse 5′CCT CCT CAA TTA TTT TTT CT3′. EVH1-binding motifs were removed by site-directed PCR mutagenesis using two

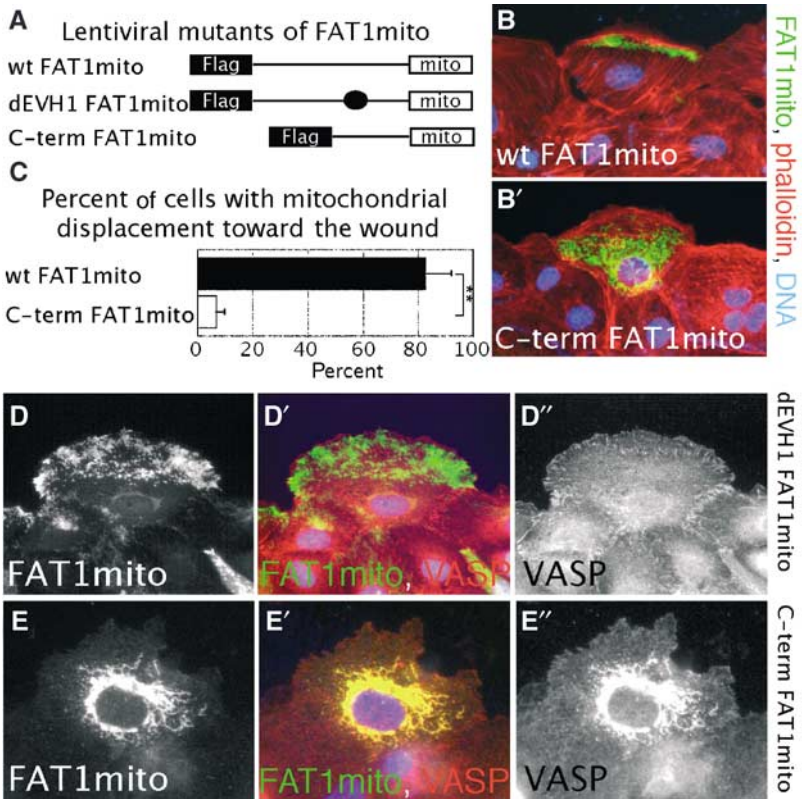

Figure 9 FAT1mito-decorated mitochondria are displaced in a polarized fashion independently of Ena/VASP interaction. (**A**) Schematic of lentiviral constructs used to express various mutants of FLAG-tagged FAT1CD targeted to outer mitochondrial membrane: wtFAT1mito, wild-type full-length FAT1 cytoplasmic domain; dEVH1-FAT1mito, FAT1mito lacking both EVH1-binding motifs; C-term FAT1mito, C-terminal half of wtFAT1mito; red oval specifies location of EVH1-binding motifs. (**B, B′**) NRK-52E cell monolayers transduced with wtFAT1mito and wounded after 48 h. FAT1mito-decorated mitochondria were invariably displaced toward denuded area in cells along the wound edge. In contrast, normal perinuclear distribution of mitochondria was observed in C-term FAT1mito-transduced cells. (**C**) A total of 50 cells each were evaluated in three independent experiments and characterized as 'displacement toward the wound' or not ($P<0.05$, ANOVA). (**D–D″**) Mitochondrial dislocation occurred independently of Ena-VASP in cells transduced with dEVH1-FAT1mito. (**E–E″**) Mitochondrial displacement did not occur in FAT1 mutants that lacked the N-terminal half of FAT1 cytoplasmic domain, while Ena/VASP recruitment was preserved.

primers delEVH1p.rev 5′P-CGC TTC AAT GTC ATA ACC CCC A3′ and delEVH1p.fwd 5′P-GAT CCC AGG GAC ATG CCT GCA3′ as described (Makarova *et al*, 2000).

The clone VASP-GFP was a gift of Dr E Fuchs (Vasioukhin *et al*, 2000); the EVH1 domain of human VASP (aa 1–114) was isolated from IMAGE clone #824217 (GenBank Acc#: AA491171) and cloned as an *Xba*I/*Hin*dIII fragment into pGSTag. Arp3GFP was a gift of Dr Schafer (Welch *et al*, 1997).

Antisera preparation

Anti-FAT1GST polyclonal antiserum was raised in rabbits against the recombinant cytoplasmic domain of mouse FAT1 fused to GST (FAT1-GST; C-terminal 385 aa of mouse FAT1 derived from IMAGE clone #4486159). Antiserum was purified by ammonium sulfate precipitation followed by two-step affinity chromatography on a GST column and a FAT1-GST column. Anti-FAT1PDZ antiserum was raised in rabbits against a synthetic peptide KLH-conjugated YESGDDGHFEEVTIPPLDSQ (aa 4563–4583, GenBank Acc#: AJ250768).

Cell culture

Cell lines were purchased from American Type Culture Collection, VA: immortalized hippocampal cells (HN33), NRK-52E (#CRL-1571). Cells were cultured in Dulbecco's modified Eagle's medium (DMEM) supplemented with 10% fetal calf serum (Life Technologies Inc.), penicillin, and streptomycin (Boehringer Mannheim). Transfections were performed using FUGENE-6 (Boehringer Mannheim). IF studies were performed according to standard protocols. Briefly, cells were fixed in 4% paraformaldehyde for 15 min and permeabilized with 0.1% Triton X-100 for 2 min or in acetone:methanol (1/1 vol) for 2 min and blocked with 10% goat serum. Primary antibodies were gifts from indicated investigators or obtained commercially and used at indicated dilutions: anti-FAT1 (Dr Eishin Yaoita, Niigata University, Niigata, Japan, 1/200), anti-FAT1GST (IF: 1/600–1/50 000; Western blot (WB): 1/2000), anti-FAT1PDZ (IF: 1/400; WB: 1/2000), anti-NWASP (Dr T Takenawa, Institute of Medical Science, University of Tokyo, Japan, 1/200), anti-Mena (Dr F Gertler, Massachusetts Institute of Technology, Cambridge, MA, 1/200), anti-Mena (clone21, BD Transduction Labs, 1/50), anti-VASP (clone 43, BD Transduction Labs, 1/100), anti-VASP (M4, ImmunoGlobe, 1/400), anti-ZO1-1A12 (Zymed Laboratories Inc., 1/500), anti-human vinculin (Sigma, 1/300), anti-Golgi 58K protein (Sigma, 1/100), anti-myc (9E11, Oncogene Science, 1/100), anti-HA (Sigma, 1/400), anti-Flag (M2, Sigma, 1/100–50 000). Secondary antibodies were obtained from Jackson ImmunoResearch Laboratories, phalloidin-TRITC and Hoechst 33342 (0.1 mg/ml) were from Sigma and MITOTRACK-ER® red CMXRos was from Molecular Probes. Slides were mounted on glass slides with PROLONG ANTIFADE® mounting medium (Molecular Probes). IF images were obtained with a Leica DMIRB inverted microscope and an RT slider digital camera (#2.3.1, Diagnostic Instruments Inc.) and collected with SPOT (Diagnostic Instruments Inc.) software and prepared for presentation with Adobe Photoshop®. For movies and kymography, phase-contrast time-lapse images were acquired using a $\times 25$ or $\times 60$ objective, an ASI 400E fan (Nevtek) and Openlab (Improvision) or ImageJ 1.30v (NIH, USA) software. Lamellipodia were defined as homogenous actin-based carpet-like structures in phalloidin stainings. Ruffles were identified by phase-contrast time-lapse videomicroscopy. Kymographs were generated along 1 pixel wide line regions orientated in the direction of individual protrusions as described (Bear *et al*, 2002).

RNAi

Endogenous FAT1 expression was knocked down by transient transfection of plasmid pAVU6 + 27 (kind gift of D Engelke, University of Michigan, USA) or by lentiviral transduction of pLL3.7 (kind gift of Dr Van Parijs, Massachusetts Institute of Technology, USA) expressing FAT1-specific small interfering hairpin RNA (shRNA) template under the U6 promoter (Paul *et al*, 2002; Rubinson *et al*, 2003). The shRNA template was comprised of a 22 bp sense template (T GTT TGA GTA CCG TGA ATA TGG; position 9884 of mRNA GenBank Acc# AF100960) specific for mouse and rat FAT1 (verified by BLAST search) followed by a 5 bp hinge region (TTCGT), a 22 bp antisense template, and a poly-U termination signal motif. Two alternate siRNA templates were used in this study with similar results: a 20 and 22 bp sense template (positions 6409–6431 and 8790–8810 of mRNA, respectively; GenBank Acc# AF100960) specific for mouse and rat FAT1 (verified by BLAST search) followed by a 4 bp hinge region (TTCG), the corresponding antisense templates, and a poly-U termination signal motif. For some experiments, the eGFP cassette was inactivated in pLL3.7 with an *Nhe*I/*Xho*I digest (removing the pCMV promoter). For lentiviral transduction, pLL3.7 expressing control or FAT1-specific shRNA was packaged and titered in 293T cells using a four-plasmid system as described (kind gift of Dr Trono, University of Geneva, Switzerland; Rubinson *et al*, 2003). NRK-52E cells were grown to confluence for 3 days and transduced with the appropriate amounts of supernatants in 8 μg/ml polybrene (Sigma) (Rubinson *et al*, 2003). Line intensity scans generated from three random areas on each cellular leading edge in multiple randomly selected transduced cells along the wound edge were analyzed and mean VASP IF intensity was obtained using ImageJ 1.30v software (NIH, USA).

Mapping of EVH1 domains

The recruitment of endogenous VASP and Mena to mitochondria by FAT1 truncation mutants was classified into three groups: 'strong recruitment' indicated mitochondrial recruitment with cytoplasmic depletion of endogenous VASP in highly expressing cells; 'weak recruitment' indicated VASP recruitment to mitochondria that were easily detectable with no obvious cytoplasmic depletion of VASP; 'absent recruitment' classified mutants without significant VASP recruitment to mitochondria.

Protein binding assays

Farwestern assays, expression and purification of GST fusion proteins, *in vitro* binding assays (Kamberov *et al*, 2000), and immunoblotting were performed according to standard protocols as described elsewhere (Nihalani *et al*, 2001).

Acknowledgements

Work was supported by a grant from the American Heart Association, the Deutsche Fortschungsgemeinschaft (MO1082/1-1), a grant for junior scientists from the University of Heidelberg (to MJM), and from the NIH and Department of Veterans Affairs (LBH). Dr Holzman is an Established Investigator of the American Heart Association.

References

Bear JE, Svitkina TM, Krause M, Schafer DA, Loureiro JJ, Strasser GA, Maly IV, Chaga OY, Cooper JA, Borisy GG, Gertler FB (2002) Antagonism between Ena/VASP proteins and actin filament capping regulates fibroblast motility. *Cell* **109:** 509–521

Bershadsky AD, Futerman AH (1994) Disruption of the Golgi apparatus by brefeldin A blocks cell polarization and inhibits directed cell migration. *Proc Natl Acad Sci USA* **91:** 5686–5689

Ciani L, Patel A, Allen ND, ffrench-Constant C (2003) Mice lacking the giant protocadherin mFAT1 exhibit renal slit junction abnormalities and a partially penetrant cyclopia and anophthalmia phenotype. *Mol Cell Biol* **23:** 3575–3582

Cox B, Hadjantonakis AK, Collins JE, Megee AI (2000) Cloning and expression throughout mouse development of mfat1, a homologue of the *Drosophila* tumour suppressor gene fat. *Dev Dyn* **217:** 233–240

Dunne J, Hanby AM, Poulsom R, Jones TA, Sheer D, Chin WG, Da SM, Zhao Q, Beverley PC, Owen MJ (1995) Molecular cloning and tissue expression of FAT, the human homologue of the *Drosophila* fat gene that is located on chromosome 4q34–q35 and encodes a putative adhesion molecule. *Genomics* **30:** 207–223

Fradelizi J, Noireaux V, Plastino J, Menichi B, Louvard D, Sykes C, Golsteyn RM, Friederich E (2001) ActA and human zyxin harbour Arp2/3-independent actin-polymerization activity. *Nat Cell Biol* **3:** 699–707

Hinz B, Alt W, Johnen C, Herzog V, Kaiser HW (1999) Quantifying lamella dynamics of cultured cells by SACED, a new computer-assisted motion analysis. *Exp Cell Res* **251:** 234–243

Inoue T, Yaoita E, Kurihara H, Shimizu F, Sakai T, Kobayashi T, Ohshiro K, Kawachi H, Okada H, Suzuki H, Kihara I, Yamamoto T (2001) FAT is a component of glomerular slit diaphragms. *Kidney Int* **59:** 1003–1012

Kaltschmidt JA, Lawrence N, Morel V, Balayo T, Fernandez BG, Pelissier A, Jacinto A, Martinez Arias A (2002) Planar polarity and actin dynamics in the epidermis of *Drosophila*. *Nat Cell Biol* **4:** 937–944

Kamberov E, Makarova O, Roh M, Liu A, Karnak D, Straight S, Margolis B (2000) Molecular cloning and characterization of Pals, proteins associated with mLin-7. *J Biol Chem* **275:** 11425–11431

Ma D, Yang CH, McNeill H, Simon MA, Axelrod JD (2003) Fidelity in planar cell polarity signalling. *Nature* **421:** 543–547

Mahoney PA, Weber U, Onofrechuk P, Biessmann H, Bryantand PJ, Goodman CS (1991) The fat tumor suppressor gene in *Drosophila* encodes a novel member of the cadherin gene superfamily. *Cell* **67:** 853–868

Makarova O, Kamberov E, Margolis B (2000) Generation of deletion and point mutations with one primer in a single cloning step. *Biotechniques* **29:** 970–972

Mitsui K, Nakajima D, Ohara O, Nakayama M (2002) Mammalian fat3: a large protein that contains multiple cadherin and EGF-like motifs. *Biochem Biophys Res Commun* **290:** 1260–1266

Moeller MJ, Sanden SK, Soofi A, Wiggins RC, Holzman LB (2002) Two gene fragments that direct podocyte-specific expression in transgenic mice. *J Am Soc Nephrol* **13:** 1561–1567

Niebuhr K, Ebel F, Frank R, Reinhard M, Domann E, Carl UD, Walter U, Gertler FB, Wehland J, Chakraborty T (1997) A novel proline-rich motif present in ActA of *Listeria monocytogenes* and cytoskeletal proteins is the ligand for the EVH1 domain, a protein module present in the Ena/VASP family. *EMBO J* **16:** 5433–5544

Nihalani D, Meyer D, Pajni S, Holzman LB (2001) Mixed lineage kinase-dependent JNK activation is governed by interactions of scaffold protein JIP with MAPK module components. *EMBO J* **20:** 3447–3458

Nobes CD, Hall A (1999) Rho GTPases control polarity, protrusion, and adhesion during cell movement. *J Cell Biol* **144:** 1235–1244

Paul CP, Good PD, Winer I, Engelke DR (2002) Effective expression of small interfering RNA in human cells. *Nat Biotechnol* **20:** 505–508

Pistor S, Chakraborty T, Niebuhr K, Domann E, Wehland J (1994) The ActA protein of *Listeria monocytogenes* acts as a nucleator inducing reorganization of the actin cytoskeleton. *EMBO J* **13:** 758–763

Ponassi M, Jacques TS, Ciani L, ffrench Constant C (1999) Expression of the rat homologue of the *Drosophila* fat tumour suppressor gene. *Mech Dev* **80:** 207–212

Rawls AS, Guinto JB, Wolff T (2002) The cadherins fat and dachsous regulate dorsal/ventral signaling in the *Drosophila* eye. *Curr Biol* **12:** 1021–1026

Rottner K, Behrendt B, Small JV, Wehland J (1999) VASP dynamics during lamellipodia protrusion. *Nat Cell Biol* **1:** 321–322

Rubinson DA, Dillon CP, Kwiatkowski AV, Sievers C, Yang L, Kopinja J, Rooney DL, Ihrig MM, McManus MT, Gertler FB, Scott ML, Van Parijs L (2003) A lentivirus-based system to functionally silence genes in primary mammalian cells, stem cells and transgenic mice by RNA interference. *Nat Genet* **33:** 401–406

Samarin S, Romero S, Kocks C, Didry D, Pantaloni D, Carlier MF (2003) How VASP enhances actin-based motility. *J Cell Biol* **163:** 131–142

Tanoue T, Takeichi M (2004) Mammalian Fat1 cadherin regulates actin dynamics and cell–cell contact. *J Cell Biol* **165:** 517–528

Vasioukhin V, Bauer C, Yin M, Fuchs E (2000) Directed actin polymerization is the driving force for epithelial cell–cell adhesion. *Cell* **100:** 209–219

Welch MD, DePace AH, Verma S, Iwamatsu A, Mitchison TJ (1997) The human Arp2/3 complex is composed of evolutionarily conserved subunits and is localized to cellular regions of dynamic actin filament assembly. *J Cell Biol* **138:** 375–384

Wu Q, Maniatis T (2000) Large exons encoding multiple ectodomains are a characteristic feature of protocadherin genes. *Proc Natl Acad Sci USA* **97:** 3124–3129

Yang CH, Axelrod JD, Simon MA (2002) Regulation of Frizzled by fat-like cadherins during planar polarity signaling in the *Drosophila* compound eye. *Cell* **108:** 675–688